AM-Loading of Fluorescent Ca^{2+} Indicators Into Intact Single Fibers of Frog Muscle

Mingdi Zhao, S. Hollingworth, and S. M. Baylor
Department of Physiology, University of Pennsylvania School of Medicine, Philadelphia, Pennsylvania 19104-6085 USA

ABSTRACT The AM loading of a number of different fluorescent Ca^{2+} indicators was compared in intact single fibers of frog muscle. Among the 13 indicators studied, loading rates (the average increase in the fiber concentration of indicator per first 60 min of loading) varied ~100-fold, from ~3 μM/h to >300 μM/h (16°C). Loading rates were strongly dependent on the molecular weight of the AM compounds, with the rate increasing steeply as molecular weight decreased below ~850. Properties of $\Delta F/F$ (the Ca^{2+}-related fluorescence signal observed with fiber stimulation) were also measured in AM-loaded fibers and compared with those previously reported for fibers microinjected with indicator. In general, the time course of $\Delta F/F$ was very similar with AM-loading and microinjection; however, the amplitude of $\Delta F/F$ was usually smaller with AM-loading. There was a strong correlation between the rate of indicator loading and the value of the parameter f (the ratio of the amplitude of $\Delta F/F$ in AM-loaded versus microinjected fibers). For indicators with small loading rates (<10 μM/h, $N = 5$), f values were generally small (≤ 0.4, $N = 4$); whereas with large loading rates (>100 μM/h, $N = 4$), f values were large (≥ 0.8, $N = 4$). This suggests that, with any AM indicator, a small concentration may associate nonspecifically with the fiber (either the indicator is incompletely de-esterified or, if completely de-esterified, not located in the myoplasmic compartment). If the loaded concentration is small, the nonspecific indicator will present a significant source of error in the estimation of $[Ca^{2+}]_i$.

INTRODUCTION

Fluorescent indicators have been widely used to study the cytoplasmic free $[Ca^{2+}]$ concentration ($[Ca^{2+}]_i$) of many cell types. With an intact cell, two principal techniques are available for introduction of the indicator into the cytoplasm: 1) injection of the permanently charged form of the indicator through a micropipette, and 2) addition of the AM-ester form to the bath where, following its diffusion across the surface membrane, intracellular esterases carry out de-esterification to the permanently charged form (Tsien, 1981). With injection, it is possible to rapidly introduce relatively large concentrations of indicator and, because the indicator is permanently charged, its rate of transport out of the cell or into intracellular organelles is expected to be small. On the other hand, the use of a micropipette risks the possibility of cell damage and, with a large cell, long waiting times may be required for the indicator to diffuse throughout the measurement region of interest.

In contrast, with the AM-loading technique, introduction of indicator is noninvasive and the cytoplasmic concentration of indicator is expected to be uniform. However, the loaded concentration of indicator may be small, and a significant fraction of the indicator's fluorescence may arise from AM indicator that has adhered extracellularly to the basement membranes or plasma lemma, or from de-esterified indicator that has been trapped within intracellular organelles (Almers and Neher, 1985). If so, quantitative estimation of $[Ca^{2+}]_i$ will be subject to substantial error.

Because of the latter problem, most studies of $[Ca^{2+}]_i$ carried out on intact single fibers of skeletal muscle have relied on the microinjection technique. At least three studies, however, have utilized AM-loading—one in mammalian fibers with the high-affinity indicator, fura-2 (Westerblad and Allen, 1991), one in amphibian fibers with fluo-3 (Caputo et al., 1994), and one in amphibian fibers with two lower-affinity indicators, furaptra and mag-fura-5 (Claflin et al., 1994). Because of the potential advantages of the AM-loading technique for some studies, we began pilot measurements of $[Ca^{2+}]_i$ in frog single fibers with AM indicators. It soon became clear that, under fixed experimental conditions, the rate of AM loading varied widely among different indicators. For example, the loading rate for furaptra was ~40-fold larger than that for fura-2.

Because of this large difference, we decided to systematically quantify loading rates of a number of different AM indicators in the hope of elucidating possible reasons for the underlying difference in rates. The results indicate that there was little correlation between loading rate and the total number of AM esters on the indicator. In contrast, there was a strong negative correlation between loading rate and the molecular weight of the AM compound. Moreover, a strong positive correlation was observed between the extent of AM loading and the extent to which the amplitude of the indicator's Ca^{2+}-related signal after loading was similar to that after microinjection. The latter correlation is explained if, with any AM indicator, a small concentration of the compound associates with the fiber in a nonspecific way; for example, some of the indicator may be either incompletely de-esterified or, if completely de-esterified, located in a cell compartment other than the cytoplasm.

Received for publication 20 September 1996 and in final form 20 January 1997.

Address reprint requests to Dr. S. M. Baylor, Department of Physiology, University of Pennsylvania School of Medicine, Philadelphia, PA 19104-6085. Tel.: 215-898-5559; Fax: 215-573-5851; E-mail: baylor@mail.med.upenn.edu.

0006-3495/97/06/2736/12 $2.00

A preliminary account of the results was presented to the Biophysical Society (Zhao et al., 1995).

MATERIALS AND METHODS

Of the 13 compounds used in this study, 12 were purchased from Molecular Probes, Inc. (Eugene, OR), whereas fura-2-FF was purchased from Teflabs (Austin, TX). The compounds fall into two general categories (Table 1): 1) tricarboxylate indicators, which have a minimum of three AM esters (column 5 of Table 1), and 2) tetracarboxylate indicators, which have a minimum of four AM esters. Tricarboxylate indicators are inherently less selective for Ca^{2+} over Mg^{2+} than are tetracarboxylate compounds, and have relatively low affinity for Ca^{2+}, with in vitro dissociation constants (K_D) in excess of 6 μM (column 3 of Table 1). Of the seven tetracarboxylate compounds studied, quin-2, fura-2, fura-red, and fluo-3 have a relatively high affinity for Ca^{2+} (in vitro K_D < 0.6 μM), whereas BTC, calcium-orange-5N, and fura-2-FF have relatively low affinity.

Procedures for fiber preparation and AM loading of indicator

Previous publications from this laboratory have described the general procedures for fiber preparation and the recording of optical signals (e.g., Baylor and Hollingworth, 1988; Konishi et al., 1991; Zhao et al., 1996). Briefly, a single twitch fiber was isolated from either the semitendinosus or ileofibularis muscle of *Rana temporaria*, mounted in a temperature-controlled chamber on a horizontal optical bench apparatus, and stretched to a relatively long sarcomere length (3.3–4.3 μm). All fibers were checked periodically for the presence of normal all-or-none responses to electrical stimulation; fibers were included in the analysis only if they responded throughout the experiment with a normal-sized second component of the intrinsic birefringence signal (Baylor and Oetliker, 1975); indicative of a normal underlying myoplasmic Ca^{2+} transient. The Ringer's solution used in the experiments contained (in mM): 120 NaCl, 2.5 KCl, 1.8 $CaCl_2$, 5 PIPES (piperazine-*N*,*N*′-bis[2-ethanesulfonic acid]) (pH 7.1). At the beginning of an experiment, this solution was exchanged for an "AM Ringer solution," which contained the same concentration of salts but also 4–20 μM of the AM-form of an indicator plus 0.1–0.4% DMSO. In some experiments, the AM Ringer's solution also contained 0.03–0.05% Pluronic (Molecular Probes, Inc.). Because AM esters have generally low solubility in aqueous media, the AM Ringer's was prepared by slow addition, with stirring, of the appropriate volume of a concentrated stock (4–20 mM AM indicator in 100% DMSO, sometimes with and sometimes without Pluronic).

During and after exposure of the fiber to AM Ringer's, the fiber's fluorescence intensity was excited periodically by light from one of two sources—either a 100-W tungsten-halogen source or a 75-W xenon source (for measurements at excitation wavelengths >400 nm or <400 nm, respectively). The excitation wavelengths (λ_{ex}) were selected by an interference filter of 10–30 nm band-pass; λ_{ex} denotes the center wavelength of the band. The emission wavelengths were selected by another interference filter (80–120 nm band-pass); λ_{em} denotes the cut-on wavelength of this band. Column 6 of Table 1 lists the values of λ_{ex} and λ_{em} used with the different indicators.

The standard temperature of the bath was 16°C, both during and after the loading period. (See, however, the note in Table 2 about two experiments with fura-2, in which loading was carried out at 25°C.) With the indicators that loaded poorly (such as fura-2), some experiments were also carried out with a somewhat higher AM concentration of indicator in the bath, e.g., 20 μM rather than 10 μM; however, no obvious effect on the rate of loading was observed at the higher concentration. Similarly, no obvious difference in loading rate was observed in the experiments that contained Pluronic in the loading solution.

Estimation of fiber-related indicator fluorescence intensity

In Results, fluorescence intensity is reported in millivolt units (proportional to intensity), as sampled from the output of the current-to-voltage circuit of

TABLE 1 Indicator properties and wavelength selections

Indicator (1)	Molecular Weight of AM-form (2)	K_D in vitro (μM) (3)	Charge on free-acid form (4)	Number of ester groups (5)	$\lambda_{ex}/\lambda_{em}$ (nm) (6)	Extinction coefficient (10^4 M^{-1} cm^{-1}) (7)
Tricarboxylates						
furaptra	723	44	−4	4	410/480	−0.41, $\Delta\epsilon$(420)
mag-fura-5	737	31	−4	4	410/480	−0.38, $\Delta\epsilon$(420)
mag-fura-red	810	55	−3	5	480/550	1.76, ϵ(450)
magnesium green	1026	7	−5	5	480/510	7.20, ϵ(500)
magnesium orange	958	43	−3	3	525/590	3.70, ϵ(540)
mag-indo-1	731	29	−4	4	410/480	−1.35, $\Delta\epsilon$(380)
Tetracarboxylates						
BTC	980	26	−4	4	480/510	3.33, ϵ(470)
calcium-orange-5N	1268	55	−4	4	525/590	6.74, ϵ(550)
fluo-3	1130	0.51	−5	5	480/510	5.96, ϵ(500)
fura-2	1002	0.19	−5	5	410/480	−0.32, $\Delta\epsilon$(420)
fura-2-FF	1038	18	−5	5	410/480	−0.50, $\Delta\epsilon$(420)
fura-red	1089	0.36	−4	6	480/550	−1.58, $\Delta\epsilon$(420)
quin-2	830	0.13	−4	4	380/480	−0.30, $\Delta\epsilon$(380)

Column 1 lists the indicators studied in this article (tricarboxylates, part A; tetracarboxylates, part B). Columns 2–5 list, respectively, the molecular weight of the AM form, the indicator's in vitro dissociation constant for Ca^{2+} measured in a salt solution, the net charge on the fully de-esterified form, and the number of AM ester groups on the parent compound. For quin-2, the value of K_D was taken from the literature of molecular probes. For the other indicators, K_D values were measured at 0 [Mg^{2+}], 0.10–0.15 M ionic strength, pH 7.0–7.1, 16–20°C, as described in Konishi et al. (1988, 1991), Kurebayashi et al. (1993), Harkins et al. (1993), and Zhao et al. (1996); for fura-2-FF, the value of K_D was measured for this article. Column 6 gives the wavelength selections for each indicator's in vivo fluorescence measurements (cf. Table 2); λ_{ex} and λ_{em} denote excitation and emission wavelengths, respectively (see Materials and methods). Column 7 lists the extinction coefficients, $\epsilon(\lambda)$ or $\Delta\epsilon(\lambda)$, used to convert indicator absorbance measurements in vivo at wavelength λ to the myoplasmic concentration of indicator.

the photo-diode recording system at a standard gain (feedback resistance = 1 Gohm). The loading of indicator into a fiber was monitored as a time-dependent increase in either F (the fluorescence intensity of the fiber at rest), or ΔF (the change in fluorescence intensity of the fiber due to a single stimulated action potential). The standard procedure was to monitor F and/or ΔF every 5–10 min, both during the period of indicator loading (1–4 h) and for an additional period (usually 1–2 h) after return of the fiber to normal Ringer's solution. Both during and after loading, any ΔF signal that was Ca^{2+}-related necessarily came from the fiber. However, raw values of resting intensity included contributions both from the fiber's fluorescence and from two extraneous sources: 1) fluorescence intensity from AM indicator in the bath, and 2) "cross-talk" (nonfluorescent) intensity, which arose from overlap of the band-passes of the excitation and emission filters. (Another potential source of interference—intrinsic fluorescence of the fiber—was negligible.) As described in Results, the non-fiber-related offset to resting intensity due to the extraneous sources was estimated in each experiment and subtracted from the raw measurements to yield the reported values of fiber-related fluorescence (i.e., F). Separate measurements of the offset were always made during the loading period, when interference from the AM indicator was large, and after return of the fiber to normal Ringer's, when interference from the AM indicator was small.

Methods of estimation of intracellular indicator concentration

After completion of loading and return of the fiber to normal Ringer's, the loaded concentration of indicator was estimated with Beer's law and a measurement of the indicator-related absorbance of the fiber. An absorbance rather than fluorescence method for the estimation of concentration was preferred, because there is evidence that many indicators bind heavily to intracellular constituents (e.g., Zhao et al., 1996) and that this binding affects fluorescence calibrations to a greater extent than absorbance calibrations (e.g., Konishi et al., 1988).

With 7 of the 13 indicators (the ones with values listed for $\Delta\epsilon$ in column 7 of Table 1), ΔA (the change in indicator-related absorbance triggered by an action potential; see Fig. 2 described in Results) was measured. Δ[CaD] (the change in the myoplasmic concentration of Ca^{2+}-indicator complex) was then calculated with the formula

$$\Delta[\mathrm{CaD}] = \Delta A/(\Delta\epsilon\,\ell). \quad (1)$$

In Eq. 1, $\Delta\epsilon$ denotes the change in the extinction coefficient of the indicator upon binding Ca^{2+}, and ℓ denotes the optical path length through myoplasm. $\Delta\epsilon$ was determined from the in vitro absorbance spectra of the indicator at the wavelength of the in vivo ΔA measurement (cf. column 7 of Table 1), which was generally close to λ_{ex} (cf. column 6 of Table 1). ℓ was determined from the fiber diameter (d) and a geometrical correction factor (p), which depended on the ratio of the diameter of the beam used for the ΔA measurement and the diameter of the fiber (see Baylor et al., 1986). For most measurements, the value of p was close to 1.0 (range, 0.92–0.97). The formula relating ℓ, d, and p is

$$\ell = 0.7pd. \quad (2)$$

The factor 0.7 is the estimated fraction of the fiber volume occupied by the myoplasmic solution (Baylor et al., 1983). As illustrated in connection with Figs. 1–3, the value of $[D_T]$ (the indicator concentration referred to the myoplasmic water volume) could then be calculated from 1) the estimated value of Δ[CaD], 2) the measured value of $\Delta F/F$, and 3) the in vitro value of $(\Delta F/F)_{max}$ (the fractional change in the fluorescence of the indicator upon switching between the Ca^{2+}-free and Ca^{2+}-bound forms). For example, with $\lambda_{ex}/\lambda_{em}$ = 410/480, $(\Delta F/F)_{max}$ is −0.932 for furaptra and −0.96 for fura-2 (Baylor and Hollingworth, 1988; Konishi et al., 1991; Zhao et al., 1996).

With the other six indicators (the ones with values listed for ϵ in column 7 of Table 1), A (the indicator-related absorbance of the resting fiber) was measured, and $[D_T]$ was calculated with the formula

$$[\mathrm{D_T}] = A/(\epsilon\ell). \quad (3)$$

In Eq. 3, ϵ denotes the value of the extinction coefficient of the indicator in its Ca^{2+}-free form and ℓ is as defined above. The value of ϵ was determined from in vitro absorbance spectra of the indicator at the wavelength of the in vivo A measurement (cf. column 7 of Table 1), which was also generally close to λ_{ex}. With the high-affinity indicators, estimation of $[D_T]$ by means of Eq. 3 may involve some error, since a fraction of the indicator may be in the Ca^{2+}-bound form at rest (see Discussion).

Before use of Eqs. 1 and 3, the fiber A and ΔA measurements were corrected for the component of the measurement attributable to the fiber intrinsic absorbance (denoted A_i and ΔA_i, respectively). The correction for ΔA_i has been described previously (Hollingworth and Baylor, 1990) and is given in the legend of Fig. 2. The correction used to estimate $A_i(\lambda)$ (the fiber intrinsic absorbance at wavelength λ) from $A_i(\lambda_{ref})$ (the intrinsic absorbance measured at a longer, reference wavelength, where the indicator-related absorbance is negligible) represents a slight modification of our previous correction. The previous formula (Baylor and Hollingworth, 1990) was: $A_i(\lambda) = A_i(\lambda_{ref})(\lambda_{ref}/\lambda)^X$, where the exponent X had a small dependence on the plane of polarization of the incident beam used for the absorbance measurement. The new formula utilized an extra parameter (k) and thereby gave a slightly improved estimate of the values of $A_i(\lambda)$ from the measurement of $A_i(\lambda_{ref})$. This formula, which was derived from $A_i(\lambda)$ measurements ($420 < \lambda < 690$) in six fibers that did not contain indicator, is given by

$$A_i(\lambda) = kA_i(\lambda_{ref})(\lambda_{ref}/\lambda)^x + (1 - k)A_i(\lambda_{ref}). \quad (4)$$

From a simultaneous least-squares fit to the data from the six experiments, the values estimated for k and X were 0.19 and 4.3, respectively, for 0° light (light polarized parallel to the fiber axis), and 0.16 and 4.3 for 90° light (light polarized perpendicular to the fiber axis). From the statistics of the equation fitted to the individual experiments, the standard error of these estimates are 0.05 and 0.03, respectively, for the k values, and 0.3 and 0.4 for the X values.

Possible errors in the estimation of $[D_T]$ due to inner filtering

With the indicators that loaded well into the fibers (such as furaptra, mag-fura-5, mag-fura-red, and mag-indo-1; cf. Results), the factor relating fiber absorbance to fiber fluorescence may have decreased as loading of indicator increased (due to the "inner-filter effect"; Cantor and Schimmel, 1980). If so, there would be some error in the calibration of the indicator concentration in the fiber from the measurements of fiber fluorescence (cf. Fig. 2, described in Results). Calculations, however, indicate that, at the levels of absorbance attained, errors in the concentration estimates due to inner filtering are likely to be small (<10%; cf. the formulas given in Kurebayashi et al., 1993); no correction was made for these errors.

Statistics

Data summarizing the optical measurements are reported as mean ± SEM. The statistical significance of a difference between means was evaluated with Student's two-tailed t-test, with the significance level set at $p < 0.05$.

RESULTS

Estimation of the AM-loading rate of furaptra

Figs. 1 and 2 show results of an experiment designed to measure the rate of loading of furaptra-AM into an intact single fiber. In Fig. 1 *A*, *C*, and *D*, zero time on the abscissa marks the time at which the fiber was first exposed to

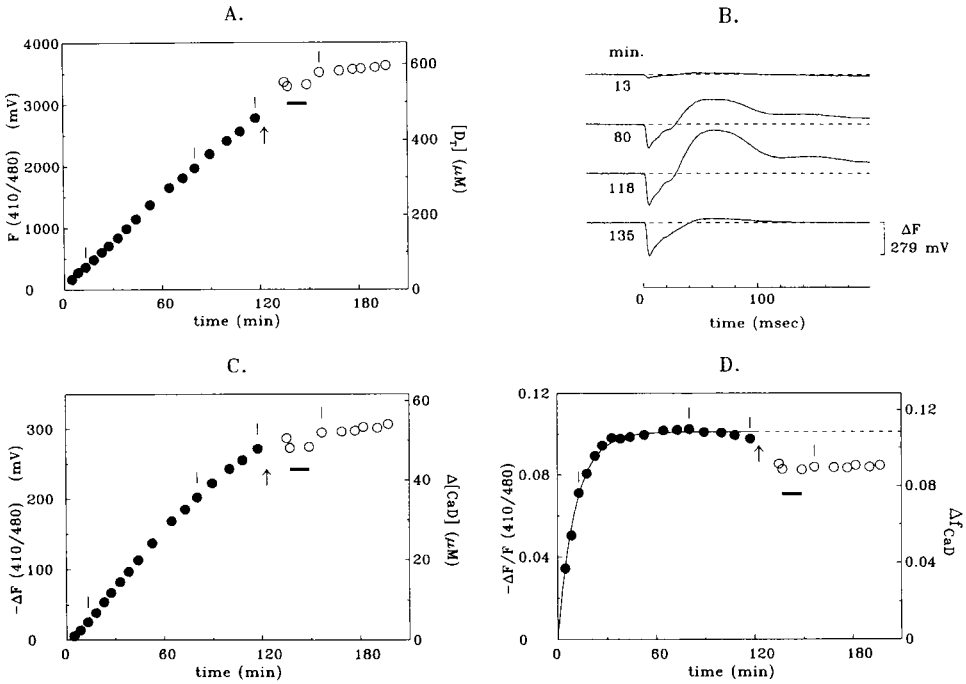

FIGURE 1 Values of furaptra-related resting F (*A*), peak $-\Delta F$ (*C*), and peak $-\Delta F/F$ (*D*) measured from a single fiber during and after exposure (*filled* and *open circles*, respectively) to 10 μM furaptra-AM plus 0.1% DMSO. (*B*) gives examples of ΔF traces recorded in response to a single action potential initiated at 0 ms; these signals were measured at the times, in min, indicated next to the traces (cf. the four vertical lines in panels *A*, *C*, and *D*). The mV units for F and ΔF are arbitrary units proportional to fluorescence intensity (see Materials and Methods). In panels *A*, *C*, and *D*, the left- and right-hand ordinates are assumed to be related by a linear scaling (cf. Results and Fig. 2). All values of F have been corrected for a constant component of intensity not related to the indicator that was associated with the fiber. The correction constant was estimated after displacement of the fiber from the optical path; the values were 853 mV for the Ringer's solution that contained furaptra-AM and 37 mV for normal Ringer's solution. In panels *A*, *C*, and *D*, the upward arrow marks the time at which the bath was washed with normal Ringer's, whereas the short horizontal bar marks the time during which furaptra-related absorbance measurements were made to estimate Δ[CaD] and $[D_T]$ (measurements and calibration procedure described in connection with Fig. 2). The curve in (*D*) is a best fit of the filled circle data with the equation $-(\Delta F/F)(t) = A \cdot [1-\exp(-t/\tau)]$, where $A = 0.101$ and $\tau = 11.3$ min. In order to reduce the size of the movement artifact observed in the falling phase of the ΔF signals [cf. the large baseline overshoots of the two middle traces in (*B*)], the fiber was stretched from a sarcomere length of 4.0 μm to 4.3 μm shortly after the bath was cleared of AM indicator. As a result of this stretch, the fiber region within the optical recording field changed slightly; because of this, and because of the change in bath composition, a small offset in the F and ΔF data [(*A*) and (*C*)] may have occurred. The final stretch (to a sarcomere length of 4.3 μm) is expected to cause a 10–15% reduction in the amplitude of $\Delta[Ca^{2+}]$ (Konishi et al., 1991). Temperature, 16°C; fiber diameter, 93 μm; sarcomere length, 4.0–4.3 μm; fiber reference, 101195.1.

furaptra-AM, which was added to the bath at a concentration of 10 μM. After ~120 min of exposure to the AM indicator, the bath was washed with indicator-free Ringer's (time marked by the *upward arrow*). Immediately after the wash, the fiber was also stretched slightly, from a sarcomere length of 4.0 to 4.3 μM, to reduce the influence of a movement artifact observed in ΔF, the indicator-related fluorescence signal recorded in response to action potential stimulation (cf. Fig. 1 *B*, described below).

In Fig. 1 *A*, the left-hand ordinate is F, the indicator-related fluorescence intensity associated with the resting fiber. During the time of exposure to furaptra-AM, there was a nearly linear increase in the measured values of F (*filled circles*; which should be approximately proportional to $[D_T]$, the indicator concentration in the fiber, referred to the myoplasmic water volume). Visual inspection of the fiber during this time revealed that the increase in F appeared to be distributed uniformly throughout the fiber. The steady increase in F is presumed to primarily reflect a steady de-esterification of furaptra-AM to charged forms of the indicator that are membrane impermeant and thus are trapped within the fiber (permanent charges of -1, -2, -3, or -4, reflecting removal of 1, 2, 3, or 4, respectively, of the ester groups from the original AM compound).

The right-hand ordinate of Fig. 1 *A* is $[D_T]$, obtained from a linear scaling of the left-hand ordinate by the calibration factor estimated from the data presented in Fig. 2 (described below). At the time the bath was cleared of AM indicator (*upward arrow* in Fig. 1 *A*), the value of $[D_T]$ was ~500 μM. Thus the average rate at which furaptra entered this fiber during the 2-h loading period was ~250 μM/h. (If calculated for the first 60-min loading period, the rate was slightly larger, ~260 μM/h.)

After removal of furaptra-AM from the bath, $[D_T]$, as expected, revealed a much smaller change with time (*open circles* in Fig. 1 *A*). The reason for the slight upward trend in these open circle data is not known with certainty. The most likely explanation is that a small concentration of AM indicator remained in the bath, due to incomplete solution exchange during the wash; thus AM indicator probably

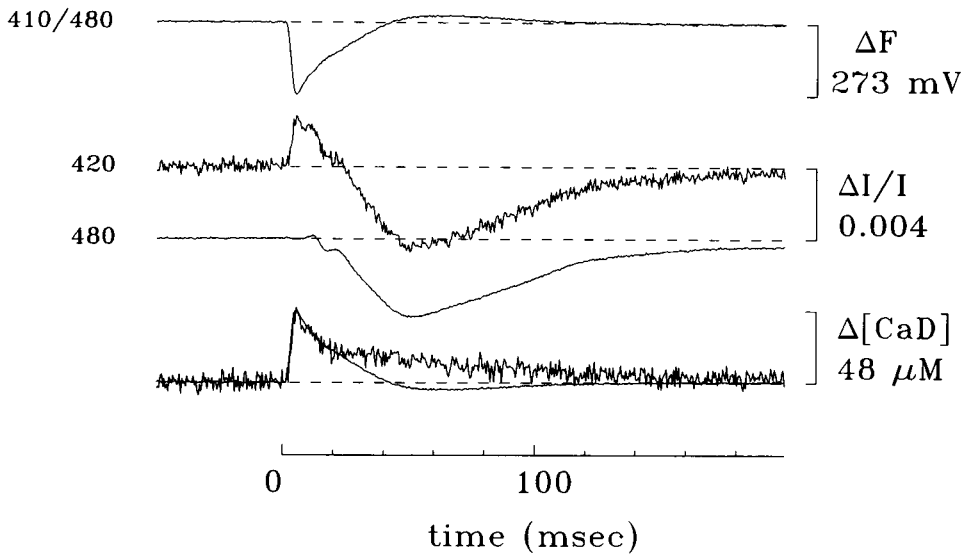

FIGURE 2 Original records of changes in fiber fluorescence (*upper trace*) and fiber transmission (traces labeled 420 nm and 480 nm) due to an action potential; the experiment is the same as shown in Fig. 1, with records taken during the time of the horizontal bar in panels *A*, *C*, and *D* of that figure. To estimate furaptra's ΔA signal, the 480 nm transmission record was scaled by the factor $(480/420)^{1.6}$ (Hollingworth and Baylor, 1990) and subtracted from the 420 nm transmission record; the resulting trace was then divided by the factor $-\log_e(10)$. The ΔA trace (noisier of the two superimposed traces at the bottom), which had a peak value of 0.00123 (not shown), was calibrated in Δ[CaD] units by Eq. 1 (see Materials and Methods); the diameter of the fiber was 93 μm. The less noisy of the two superimposed traces is the upper ΔF record but re-scaled to match the displayed amplitude of the ΔA trace.

continued to load into the fiber at a small rate. [Note: in other fibers, *F* values measured after the wash sometimes decreased with time (not shown); cf. Konishi et al., 1991.] The slightly larger value of the first open symbol in Fig. 1 *A* compared with the last filled symbol could reflect a true increase in $[D_T]$ or could reflect an error in the estimation of $[D_T]$ (see note in the legend of Fig. 1 about the change in experimental conditions associated with the solution change.)

At the time of each of the *F* measurements shown in Fig. 1 *A*, the fiber was also stimulated by an external shock to give a twitch. Fig. 1 *B* shows examples of the ΔF signal recorded as a result of this stimulation; these traces were measured at the times indicated by the four vertical lines in Fig. 1 *A*, *C*, and *D*. The first three ΔF signals in Fig. 1 *B* were obtained before the final stretch of the fiber and, beginning ~20 ms after stimulation, the later time courses of these signals, particularly the second and third ΔF traces, reveal obvious contamination by a movement artifact (cf. the large overshoot of the dashed baseline). In contrast, the fourth trace in Fig. 1 *B*, which was obtained after the final stretch of the fiber, is much less affected by fiber movement. For all four traces, the time to peak of the ΔF signal occurred 4.5–5.5 ms after stimulation and the half-width of ΔF was 10.1–12.6 ms. These times are very similar to those observed in fibers microinjected with furaptra (5.0 ± 0.1 ms for time to peak and 10.9 ± 0.7 ms for half-width; Zhao et al., 1996).

In Fig. 1 *C*, the left-hand ordinate is (minus) the peak value of ΔF, whereas the right-hand ordinate is the peak of ΔF calibrated in units of Δ[CaD], the change in the myoplasmic concentration of Ca^{2+}-indicator complex. As in Fig. 1 *A*, the calibration of the right-hand ordinate in Fig. 1 *C* was obtained from the left-hand ordinate by the method described in the next section. In Fig. 1 *C*, the peak value of Δ[CaD] increased steadily during exposure of the fiber to furaptra-AM; after removal of the AM indicator, Δ[CaD] remained almost constant at a level near that of the final measurement taken in the presence of furaptra-AM. Thus the time-dependent change in Δ[CaD] in Fig. 1 *C* was generally similar to that observed for $[D_T]$ in Fig. 1 *A*.

The *F* and $-\Delta F$ data of Fig. 1A, C were combined to give the data of Fig. 1D ($-\Delta F/F$, left-hand ordinate). Interestingly, during the early minutes of exposure to AM indicator, the $-\Delta F/F$ versus time plot had a clearly resolved rising phase. The time course of this phase was well-fitted by an exponential relaxation to a final steady level (thin curve in Fig. 1 *D*, with a time constant of 11.3 min and a final $-\Delta F/F$ level of 0.101). The presence of a rising phase implies that the indicator that first became associated with the fiber was less sensitive to $\Delta[Ca^{2+}]$ than was the indicator that became associated subsequently. This result is consistent with several possibilities. First, the AM indicator is generally hydrophobic and a small concentration of AM indicator may have quickly associated with hydrophobic sites on the exterior of the fiber or within the cell interior; such indicator would contribute to resting *F* but not ΔF. Second, it is likely that de-esterified indicator is initially trapped within the fiber in the singly charged form (−1; presumed to be Ca^{2+} insensitive) and, only with some delay, progressively converted to the more negatively charged forms (the −4 form presumed to be the principal Ca^{2+}-sensitive form).

Beginning ~30 min after the first exposure of this fiber to furaptra-AM, the filled-circle data in Fig. 1 *D* became

nearly independent of time. Thus, after this time, the fraction of total indicator associated with the fiber that was insensitive to $\Delta[Ca^{2+}]$ may have been negligible. Alternatively, this fraction may not have been negligible if the rates of accumulation of Ca^{2+}-insensitive and Ca^{2+}-sensitive indicator in the fiber were approximately constant.

After the removal of furaptra-AM from the bath, the amplitude of the $-\Delta F/F$ signal was also essentially time-independent (*open circle* data in Fig. 1 *D*). This result is consistent with the idea that a stable distribution of indicator forms had been reached within the fiber. (Note: the ~15% decrease in the peak value of $-\Delta F/F$ immediately after removal of AM indicator likely reflects a true decrease in the amplitude of $\Delta[Ca^{2+}]$ due to stretch of the fiber to the long sarcomere length—see legend of Fig. 1.)

The right-hand ordinate of Fig. 1 *D* refers the data for the peak of $-\Delta F/F$ to units of Δf_{CaD}, the change in the fraction of the indicator in the Ca^{2+}-bound form during fiber activity. Just before removal of AM indicator from the bath, peak Δf_{CaD} was ~0.107; after removal of indicator, peak Δf_{CaD} was ~0.090. Since the larger of these values is at the low end of the range observed for peak Δf_{CaD} in fibers microinjected with indicator, 0.132 ± 0.025 (mean ± SD; sarcomere lengths, 3.6–4.3 μm; Zhao et al., 1996), these data suggest that Δf_{CaD} might be smaller with AM loading than with microinjection. If so, at least three possibilities could account for this result. First, as mentioned above, some of the indicator associated with the fiber might still have been in the original AM form (bound to hydrophobic sites on the fiber). Second, some of the permanently charged indicator trapped within the fiber may not have been completely de-esterified to the −4 form. Third, some of the indicator within the fiber, even if completely de-esterified, may have been trapped within a nonmyoplasmic compartment (thus contributing to F but not ΔF).

Estimation of Δ[CaD] and $[D_T]$ from furaptra's *F*, *ΔF*, and *ΔA* signals

Fig. 2 shows three other optical traces recorded during fiber activity from the experiment of Fig. 1. These traces, which were taken shortly after removal of AM indicator from the bath (during the time indicated by the horizontal bars in Fig. 1), illustrate the method used to calibrate the right-hand ordinates of Fig. 1, *A* and *C* from the corresponding left-hand ordinates. The top trace shows ΔF, which had a peak value of −273 mV, a time-to-peak of 5.5 ms, and a half-width of 12.4 ms. The second and third traces show $\Delta I/I$, the fractional transmission change (proportional to ΔA), recorded with 420 nm and 480 nm light, as indicated. With 420 nm light, the $\Delta I/I$ signal is expected to reflect both furaptra's ΔA and the fiber's intrinsic ΔA; whereas, with 480 nm light, the signal should be free of a furaptra-related ΔA. Additionally, $\Delta I/I$ traces are generally quite sensitive to movement artifacts, and a substantial movement artifact clearly began in both $\Delta I/I$ traces ~20 ms after stimulation (cf. the large undershoots of the baseline). To obtain an estimate of the furaptra-related ΔA, the 480-nm trace was scaled and subtracted from the 420-nm trace (see legend of Fig. 2); the resultant trace is shown at the bottom of Fig. 2 as the noisier of the two superimposed traces. As indicated by the calibration bar at the lower right, the peak amplitude of this ΔA signal (0.00123; not shown) is explained by a peak value of Δ[CaD] of 48 μM. The less noisy superimposed trace is a scaled version of the ΔF signal, displayed so as to have the same peak value as the Δ[CaD] trace. As expected, aside from errors attributable to the movement artifact, the time courses of these two traces are identical. From the relative amplitude of the traces before onset of the movement artifact, the scaling factor was determined that related ΔF to Δ[CaD], namely, $\Delta[CaD]/\Delta F = -0.177$ μM/mV. This factor was assumed to apply at all times during the experiment, and thus the calibration of the right-hand ordinate in Fig. 1 *C* was obtained from the left-hand ordinate.

As described in Zhao et al. (1996), a peak value of furaptra's Δ[CaD] signal in combination with a peak value of $-\Delta F/F$ permits estimation of $[D_T]$. Thus, at the time of the measurements of Fig. 2, when peak Δ[CaD] was 48 μM and peak $\Delta F/F$ was −0.083, a $[D_T]$ of 541 μM is estimated $(-0.932 \cdot \Delta[CaD] \cdot (\Delta F/F)^{-1}$, the factor −0.932 being specific for a λ_{ex} of 410 nm). As for Fig. 1 *C*, the scaling factor relating F and $[D_T]$ at the time of the measurements of Fig. 2 (0.165 μM/mV) was assumed to apply throughout the experiment, thus giving the calibration of the right-hand ordinate in Fig. 1 *A*.

Summary of data from the furaptra-AM loading experiments

In Table 2, the first row summarizes results from six furaptra experiments analyzed by the method illustrated in Figs. 1 and 2. This analysis, if referred to the data collected during the first 60 min of exposure to AM indicator, gave an average rate of increase of $[D_T]$ of 312 ± 50 μM/h (mean ± SEM; column 2 of Table 2). In three experiments in which furaptra loading was continued for 2–3 h, there was little evidence that the loading rate slowed substantially with time (cf. Fig. 1). No correlation was observed between loading rate and fiber diameter (range, 60–138 μm; not shown).

As indicated by the agreement between columns 5 and 8 of Table 2, the time course of the furaptra ΔF signal in AM-loaded fibers was very similar to that observed previously in microinjected fibers. The average amplitude of $\Delta F/F$ in AM-loaded fibers, however, was only 0.8 times that in microinjected fibers (cf. columns 4 and 7 of Table 2). Although the difference between the numbers in columns 4 and 7 is not quite statistically significant ($p = 0.073$), this difference, as mentioned earlier, is in the direction expected if a minor fraction of the AM-loaded furaptra was in a

TABLE 2 Analysis of indicator signals following AM loading or microinjection into single muscle fibers

Indicator (1)	loading rate (μM/h) (2)	$\Delta F/F$ (AM-loaded) N (3)	Peak ($\Delta F/F$) (4)	Half-width (ms) (5)	$\Delta F/F$ (micro-injected) N (6)	Peak ($\Delta F/F$) (7)	Half-width (ms) (8)	f (4)/(7) (9)
Tricarboxylate indicators								
furaptra	312 ± 50	6	−0.105 ± 0.015	12.7 ± 1.1	12	−0.132 ± 0.007	10.9 ± 0.7	0.80
mag-fura-5	382 ± 96	3	−0.132 ± 0.008	10.8 ± 1.1	2	−0.119 ± 0.003	9.8 ± 1.5	1.11
mag-fura-red*	110 ± 17	6	−0.077 ± 0.010	8.3 ± 1.3	7	−0.074 ± 0.008	5.8 ± 0.2	1.04
magnesium green	2.7 ± 0.9	2	0.200 ± 0.014	15.5 ± 2.2	4	0.507 ± 0.065	22.6 ± 2.5	0.39§
magnesium orange	2.9 ± 0.3	3	0.052 ± 0.007	20.6 ± 0.4	3	0.145 ± 0.024	12.5 ± 2.5	0.36§
mag-indo-1	377 ± 26	3	−0.096 ± 0.005	14.9 ± 1.9	3	−0.114 ± 0.010	11.6 ± 2.3	0.84
Tetracarboxylate indicators								
BTC	15 ± 7	2	−0.006 ± 0.002	11.8 ± 2.5	6	−0.072 ± 0.006	16.2 ± 1.0	0.08§
calcium-orange-5N	34 ± 10	4	0 ± 0	—	5	0.260 ± 0.041	16.8 ± 1.5	0§
fluo-3	8.4 ± 2.0	2	1.463 ± 0.530	42.8 ± 0.1	4	7.30 ± 1.100	46.8 ± 3.8	0.20§
fura-2#	8.2 ± 3.5	4	−0.521 ± 0.034	76.1 ± 6.7	3	−0.683 ± 0.032	53.4 ± 5.1	0.76§
fura-2-FF	43 ± 3	2	−0.080 ± 0.025	30.6 ± 5.7	2	−0.134 ± 0.014	16.4 ± 2.8	0.60
fura-red	<10	3	−0.074 ± 0.016	71.0 ± 11.3	3	−0.412 ± 0.041	63.1 ± 3.7	0.18§
quin-2	55 ± 27	2	−0.170 ± 0.027	109.6 ± 32.4	2	−0.235	53.4 ± 5.1	0.72

Column 1 lists the indicators, column 2 their average rate (mean ± SEM) of loading into frog fibers during the first 60 min of exposure to AM indicator (16°C), and column 3 the corresponding number of AM loading experiments. Columns 4 and 5 give the average values for peak and half-width of the $\Delta F/F$ signals after AM loading, whereas columns 7 and 8 give analogous values after microinjection of indicator (see Zhao et al., 1996); the bath temperature during the measurements of columns 4–5 was always 16°C. Column 6 gives the number of microinjection experiments. Column 9 gives the parameter f (discussed in the text), the ratio of column 4 to column 7.

*With mag-fura-red, the values for peak and half-width refer to the first component (i.e., the component thought to directly depend on $\Delta[Ca^{2+}]$) of the 2-component signal seen with this indicator (Zhao et al., 1996).

#With fura-2, the bath temperature during loading was 16°C in 2 of the experiments (loading rates of 4.1 and 4.1 μM/hour) and 25°C in the other 2 experiments (loading rates of 6.1 and 18.5 μM/hour).

§Average values in columns 4 and 7 are significantly different.

molecular form that was either insensitive to $\Delta[Ca^{2+}]$ or associated with a cell compartment that did not see $\Delta[Ca^{2+}]$.

Estimation of the AM-loading rate of fura-2

Fig. 3 shows results from an analogous AM loading experiment carried out with an indicator (fura-2) that had a much smaller rate of loading than furaptra. Because the loading rate was so much smaller, less complete information was obtained about fura-2's loading time course. First, although we presume that fura-2's resting F values increased progressively during the loading period, an increase was not in fact resolved above the noise in the F measurements; this noise was caused by fluctuations in background fluorescence due to slow variations in lamp output. Because F values were unreliable during the loading period, filled circle data have been omitted from the plot in Fig. 3 *A*. [Note: with 10 μM fura-2-AM in the bath, the background fluorescence averaged ~970 mV, and fluctuations in background fluorescence averaged ~40 mV.] After removal of fura-2-AM (*upward arrow* in Fig. 3 *A*, at time = 245 min), background fluorescence and its fluctuations became much smaller (average values of 33 mV and 1 mV, respectively); thus resting F could be determined fairly reliably. These values are shown as the open circles in Fig. 3 *A*. Second, because the amount of fura-2 that loaded into the fiber was small and because the $\Delta I/I$ signal from this fiber had a relatively large movement artifact, it was not possible to accurately estimate the indicator-related ΔA signal; thus, in contrast to the furaptra measurements illustrated in Fig. 2, the scaling factor required to convert ΔF to Δ[CaD] could not be determined by measurements from this fiber alone. This conversion was instead based on measurements obtained in another fura-2-AM experiment (not shown; data described below), in which interference from movement artifacts was smaller.

As shown in Fig. 3 *B*, the peak of the ΔF signals in this fura-2 experiment appeared to be reliably resolved, both during and after exposure to AM indicator. As in Fig. 1, the progressive increase in the amplitude of ΔF with loading time is presumed to reflect a steady accumulation within the fiber of the fully de-esterified form of the indicator (permanent charge of −5) due to the steady activity of intracellular esterases. The traces in Fig. 3 *B* also show that the time courses of the ΔF signals were similar throughout the experiment, although the time courses of the smaller ΔF signals (corresponding to shorter loading times) may have been influenced somewhat by a movement artifact. In this experiment, the average values for time-to-peak and half-width of ΔF were 17.6 ms and 56.6 ms, respectively. These values observed with AM-loading are very similar to those observed after microinjection of fura-2 (14.7 ± 1.4 ms and 53.4 ± 5.1 ms; Zhao et al., 1996; cf. Table 2). [Note: as reported previously for fibers microinjected with fura-2, the

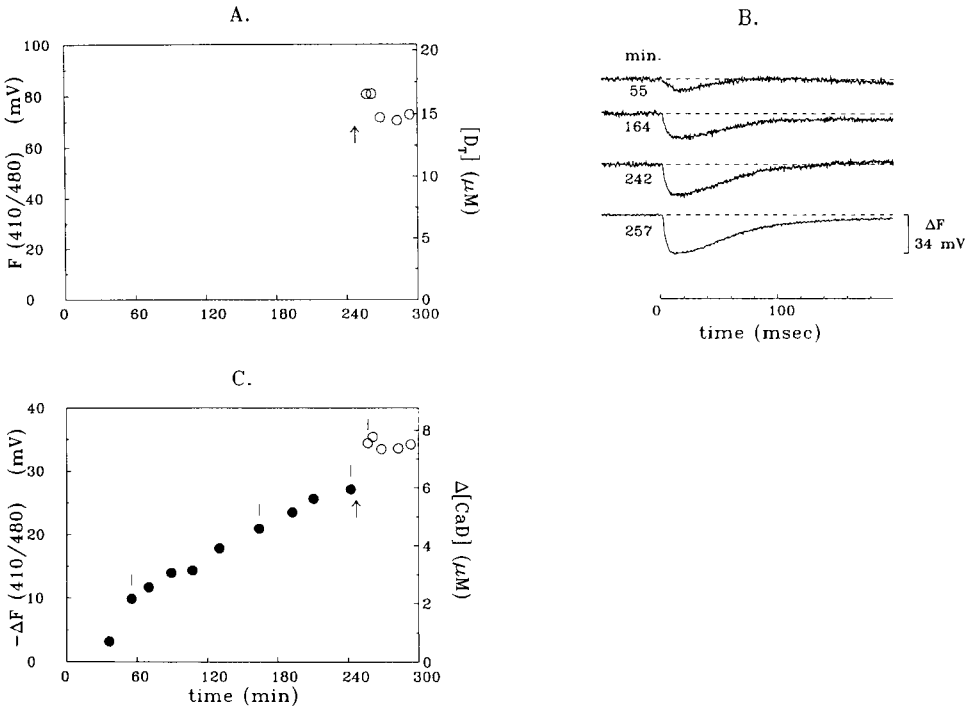

FIGURE 3 Fura-2-related resting F (A), ΔF traces (B), and peak values of $-\Delta F$ (C), measured during and after exposure (*filled* and *open circles*, respectively) of a fiber to 16 μM fura-2-AM plus 0.4% DMSO. As in Fig. 1, the upward arrows mark the time at which AM indicator was removed from the bath, whereas the four vertical lines in (C) mark the times at which the ΔF traces in (B) were taken. The diameter of the fiber was 93 μm, whereas that of the fiber used to calibrate ΔF in units of Δ[CaD] (not shown; see text) was 135 μm. The calibration factor (Δ[CaD]/ΔF) determined for the latter fiber, -0.105 μM/mV, was multiplied by the factor 2.11 (the square of the ratio of the fiber diameters) to obtain the calibration factor -0.221 μM/mV to relate the left- and right-hand ordinates of Fig. 3 C. Temperature, 16°C (both during and after loading); sarcomere length, 3.5 μm; fiber reference, 102494.1.

time course of fura-2's Ca^{2+}-related ΔF signal is substantially slower than that of furaptra's, an effect explained by the slow intracellular kinetics of the Ca^{2+}-fura-2 reaction; cf. Zhao et al., 1996.]

As mentioned above, traces analogous to those of Fig. 2 were obtained in a second fura-2-AM loading experiment, in which ΔF and ΔA measurements were made shortly after the bath was cleared of fura-2-AM. The scaling factor found to relate the amplitudes of Δ[CaD] and ΔF in this fiber was -0.105 μM/mV. This calibration factor was then adjusted for use in the other fura-2-AM experiments (that of Fig. 3 and two other experiments; see legend of Fig. 3) to calibrate Δ[CaD] from ΔF. Thus, the calibration of the right-hand ordinate of Fig. 3 C was obtained from the left-hand ordinate.

As for furaptra, a calibrated fura-2 Δ[CaD] signal in combination with a corresponding peak value of $-\Delta F/F$ permits estimation of [D_T]. At the time of the final open circle measurements of Fig. 3, A and C, (when Δ[CaD] was 7.6 μM, ΔF was -34.4 mV, and F was 72 mV), a [D_T] of 15 μM is estimated ($-0.96 \cdot \Delta[\text{CaD}] \cdot (\Delta F/F)^{-1}$; see above and Materials and Methods). Under the assumption that the amplitude of the $\Delta F/F$ signal observed in this fiber after the loading period (-0.5) also applied during loading, the value of Δ[CaD] observed at 60 min after addition of AM indicator (~2 μM) implies that the corresponding value of [D_T] was ~4 μM. Hence a loading rate of ~4 μM/h is estimated for the first 60 min of loading in this experiment. The average rate observed in four experiments with fura-2-AM was 8.2 ± 3.5 μM/h (column 2 of Table 2). This rate is ~40-fold smaller than that estimated for furaptra.

Summary of AM loading rates measured with other indicators

Based on analogous measurements of F, ΔF, and ΔA (or, alternatively, of F and A for some indicators; see Materials and Methods), rates of AM loading were estimated for five other tricarboxylate indicators and six other tetracarboxylate indicators. The results, referred to the first 60 min of loading, are tabulated in column 2 of Table 2. Examples of the $\Delta F/F$ signals recorded after AM loading of these 11 indicators are given in Fig. 4. It should be noted that the relative signal-to-noise ratio of the ΔF signals in Fig. 4 depends not only on [D_T] and the amplitude of $\Delta F/F$, but also on fiber diameter, the illumination intensity at λ_{ex}, the absorbance of the indicator at λ_{ex}, the quantum efficiency of fluorescence at λ_{ex}, and the band-pass of the fluorescence emission filter.

Tricarboxylate indicators

Of the six tricarboxylates examined, three indicators (furaptra, mag-fura-5, and mag-indo-1) had average loading rates that were quite large, 312–382 μM/h (column 2 of Table 2); these rates are not significantly different from each other. With mag-fura-red, the average loading rate was significantly smaller, 110 μM/h, but still substantial. In contrast, average loading rates for the other two tricarboxylate indicators (magnesium green and magnesium orange) were very small, ~3 μM/h.

Column 9 of Table 2 gives values of the parameter f, the ratio of the amplitude of $\Delta F/F$ in AM-loaded fibers (column 4) versus microinjected fibers (column 7). Interestingly, the four tricarboxylate indicators that had large loading rates

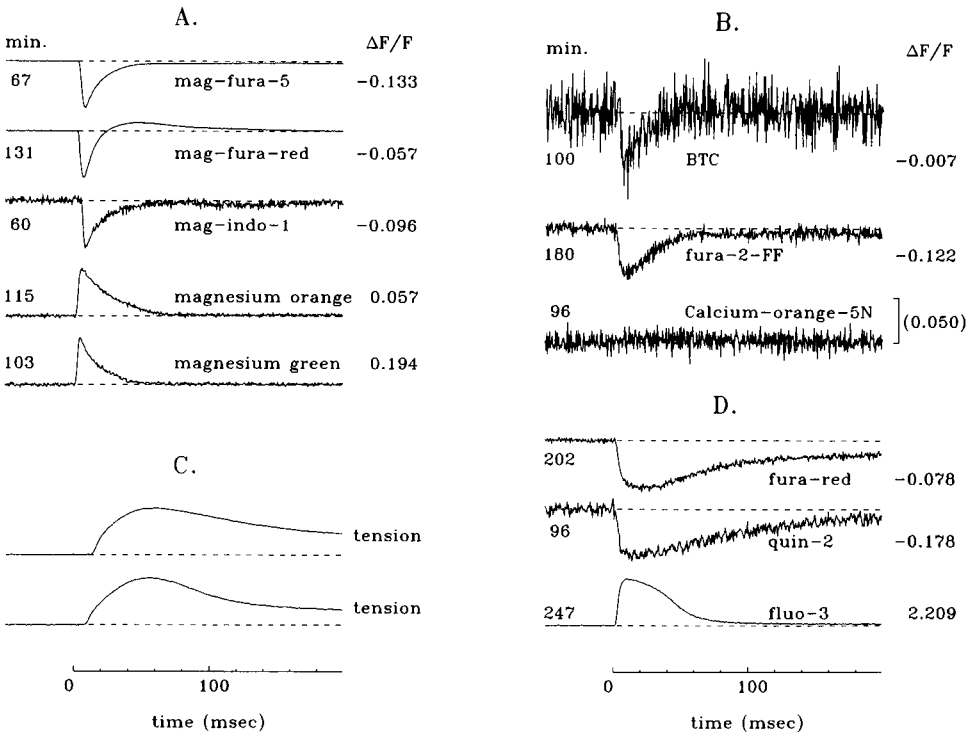

FIGURE 4 Examples of $\Delta F/F$ signals during a twitch (panels *A*, *B*, and *D*) recorded with the 11 other AM indicators used in this study; (*C*) gives representative examples of the twitch tension responses recorded simultaneously in two of the experiments (with mag-fura-red and fluo-3). (*A*) gives results for the tricarboxylate indicators, (*B*) for the lower-affinity tetracarboxylates, and (*D*) for the higher-affinity tetracarboxylates. All records were obtained after return of the fibers to normal Ringer's solution; the time (in min) that a fiber was in the loading solution is indicted to the left of each trace. The number at the right of each trace gives the peak value of $\Delta F/F$ (except for calcium-orange-5N, where the number in parentheses corresponds to the amplitude of the vertical bar). The number of sweeps averaged per trace were four for magnesium orange, two for mag-fura-red and fura-2-FF, and one for each of the other indicators. Temperature, 16°C; sarcomere lengths, 3.3–4.0 μm; fiber diameters, 66–105 μm.

also had large f values, 0.8–1.1. In contrast, the two poorly loading tricarboxylate indicators (magnesium green and magnesium orange) had much smaller f values, 0.36–0.39. Thus, for the indicators with small loading rates, a substantial fraction of resting fluorescence appears to have arisen from molecules that were either insensitive to $\Delta[Ca^{2+}]$ or located in a compartment that did not see $\Delta[Ca^{2+}]$. Because of this problem, neither magnesium green-AM nor magnesium orange-AM appears to be suited for quantitative studies of $\Delta[Ca^{2+}]$ in frog fibers. Because, however, these two indicators have a $\Delta F/F$ signal with a relatively large signal-to-noise ratio (cf. Fig. 4), they may be useful for qualitative studies of $\Delta[Ca^{2+}]$.

Tetracarboxylate indicators

Of the seven tetracarboxylates examined, three indicators (fluo-3, fura-2, and fura-red) also had average loading rates that were small (<10 μM/h). Of these, fura-2 was exceptional in that it had a reasonably large f value (0.76; measured after loading times of 182–245 min). Fura-2 also has a relatively large quantum efficiency for fluorescence, and, if the indicator was allowed to load for times substantially longer than an hour, gave ΔF signals with a large signal-to-noise ratio (cf. Fig. 3 *B*). [Note: signal-to-noise ratio with fura-2 is expected to be even larger if a λ_{ex} of 380 nm is used.] Thus, fura-2-AM has the potential for semi-quantitative use in studies of $[Ca^{2+}]_i$ in amphibian fibers.

With the other four tetracarboxylate indicators (BTC, calcium-orange-5N, fura-2-FF, and quin-2), average loading rates were moderate, 15–55 μM/h. Unfortunately, f values for BTC and calcium-orange-5N were very small, <0.1. Remarkably, with calcium-orange-5N, no significant Ca^{2+}-related signal was detected during fiber activity (cf. Fig. 4 and column 4 of Table 2.) Thus the AM forms of BTC and calcium-orange-5N are very poor candidates for even qualitative use as Ca^{2+} indicators in frog fibers. Of the two remaining indicators, both fura-2-FF and quin-2 had f values that were of reasonable size (≥0.6). These AM indicators are thus reasonable candidates for semi-quantitative use as Ca^{2+} indicators in frog fibers.

Dependence of the parameter *f* on the amount of indicator loaded

Fig. 5 plots the f values estimated for the 13 indicators (column 9 of Table 2) versus the average values of the indicator concentrations at the time that the amplitude of $\Delta F/F$ was estimated in the AM-loading experiments (which, in all cases, occurred after the removal of AM indicator

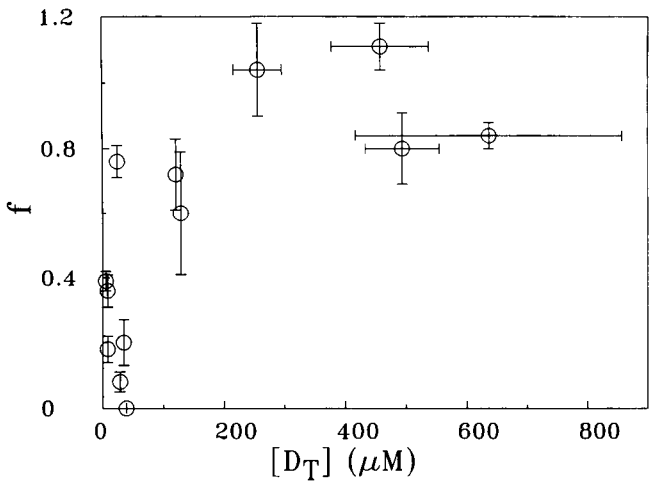

FIGURE 5 f values for the 13 indicators (column 9 of Table 2) plotted as a function of the average myoplasmic concentration of AM-loaded indicator (i.e., the concentration present at the time of the determination of the amplitude of $\Delta F/F$ in the AM-loaded fibers). The error bars denote ± SEM (unless the error bar was smaller than the symbol size, in which case it was omitted).

from the bath). This plot reveals a strong dependence of f value on extent of loading and suggests that a myoplasmic concentration >100 μM is usually required if f is to be close to 1. On the other hand, factors other than loading concentration must also influence f, since 1) with fura-2, f was nearly 0.8 in fibers that loaded to only 20–25 μM, and 2) with calcium-orange-5N, no Ca^{2+}-related signal could be measured from fibers that loaded to ~30 μM.

Dependence of the rate of AM loading on structural features of the AM compounds

With information available on loading rates of the 13 different AM indicators, it was of interest to examine whether the loading rate depended strongly on either the total number of AM esters present on, or the molecular weight of, the original AM compound. This dependence is shown in Fig. 6. Part *A* shows that there was no obvious dependence of loading rate on the number of esters. In contrast, part *B* shows that there was a striking inverse dependence on molecular weight, with loading rate increasing steeply as molecular weight decreased below ~850.

DISCUSSION

The AM loading of fluorescent Ca^{2+} indicators into cells has been widely used in the measurement of $[Ca^{2+}]_i$, and a number of authors have pointed to potential pitfalls in the estimation of $[Ca^{2+}]_i$ with AM-loaded indicator (e.g., Almers and Neher, 1985; Scanlon et al., 1987; Williams and Fay, 1990; Roe et al., 1990). Our study on frog muscle fibers is, we believe, the first to 1) quantify rates of loading of a number of different AM indicators into the same cell type, and 2) systematically compare the properties of the Ca^{2+}-related signals in AM-loaded and microinjected cells. Among the 13 indicators examined, a remarkable variability was found, both in the absolute rate of loading and in the degree to which the Ca^{2+}-related signal in AM loaded fibers was similar to that in microinjected fibers. A comparison among the tricarboxylate indicators (magnesium green and magnesium orange versus furaptra, mag-fura-5, and mag-indo-1) gives the most striking difference in loading rates: 3 μM/h versus 312–382 μM/h, respectively (column 2 of Table 2). In terms of differences in the amplitude of $\Delta F/F$ with AM loading and microinjection, a comparison of four tetracarboxylate indicators (BTC, calcium-orange-5N, fluo-3, and fura-red) versus four tricarboxylate indicators (furaptra, mag-fura-5, mag-fura-red, and mag-indo-1) gives the most striking difference: f values of 0–0.2 vs. 0.8–1.1, respectively (column 9 of Table 2). The small f values observed for BTC, calcium-orange-5N, fluo-3, and fura-red imply that a major fraction of these indicators was not in the myoplasm in the fully de-esterified form.

Overall, there was a general tendency for AM indicators that loaded poorly to have small f values (Fig. 5). This correlation suggests that, with AM loading, a small concentration (perhaps a few μM) of any indicator will associate with the fiber in a nonspecific way—e.g., either the indicator is not completely de-esterified or is not located entirely within the cytoplasm. For an indicator that loads well, a small concentration of nonspecific indicator will lead to only a minor reduction in the expected amplitude of $\Delta F/F$. For an indicator that loads poorly, however, the likely result

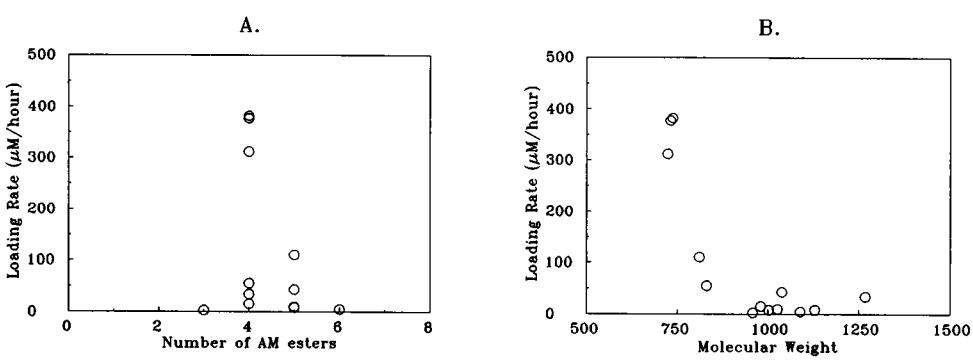

FIGURE 6 (*A*) plots, for the 13 AM compounds of this study, the estimated loading rate (ordinate; cf. column 2 of Table 2) versus the number of esters on the parent compound (abscissa; cf. column 5 of Table 1). (*B*) is analogous, with the abscissa being the molecular weight of the AM compound (column 2 of Table 1).

will be a $\Delta F/F$ signal that is smaller than expected (small f value), thus implying a potentially large error in the calibration of $[Ca^{2+}]_i$. The exact magnitude of this error will clearly vary with the choice of indicator, with loading time, and probably also with the type of cell under investigation. Thus AM loading, while potentially useful for qualitative and semi-quantitative investigations of $[Ca^{2+}]_i$, should probably not be considered a substitute for the microinjection technique, particularly in cell types that are readily amenable to microinjection and if indicators with small loading rates are to be employed.

Correlation between loading rate and indicator structure

As shown in Fig. 6 *B*, there is a strong inverse correlation between the molecular weight of an AM compound and the rate at which it loaded into frog single fibers. This correlation likely exists because, in general, the increase in molecular weight is associated with an increase in carbon-containing moieties, and hence an increase in the overall hydrophobicity of the compound. As hydrophobicity increases, the maximal theoretical concentration of AM indicator that can be dissolved within the water solution (either extracellular or intracellular) presumably decreases, and thus the concentration of AM indicator available to react with intracellular esterases presumably also decreases. Also, as hydrophobicity increases, there may be a decrease in the rate at which AM indicator can enter the intracellular water compartment as a result of partitioning into and then out of the hydrophobic exterior membranes. Thus, the maximal theoretical concentration achievable within the intracellular water solution may not be reached for a strongly hydrophobic AM compound.

The data in Fig. 6 *B* predict that AM compounds of molecular weight <850 should load reasonably well into frog muscle fibers, and findings with two other AM compounds of lower molecular weight (EGTA-AM, molecular weight = 669; BAPTA-AM, molecular weight = 765) appear to follow this pattern. Johnson and Jiang (1996) report that, following exposure of frog fibers to 20 μM EGTA-AM for 70 min (10°C), the amplitude of the tension response was reduced by a factor of 5, whereas Zhao et al. (1996; cf. their Fig. 6) report that, following exposure of a fiber to 4 μM BAPTA-AM for 160 min (16°C), the amplitude of $\Delta[Ca^{2+}]$ during a twitch was reduced ~10-fold. These reductions are likely due to the presence of millimolar or near millimolar concentrations of chelator in myoplasm (cf. Hollingworth et al., 1992).

Comparisons with other loading studies of AM-indicators into skeletal muscle fibers

There have been at least two previous studies of $\Delta[Ca^{2+}]$ and tension in intact frog single fibers exposed to AM indicators. Claflin et al. (1994) used a 30-min exposure to 5 μM furaptra-AM or mag-fura-5-AM (20°C), whereas Caputo et al. (1994) used a 60-min exposure to 10–20 μM fluo-3-AM (21°C). Although neither study quantified the myoplasmic concentration of the indicators, the concentrations achieved in both studies were clearly sufficient to yield ΔF signals with a good signal-to-noise ratio.

In a study on single fast-twitch fibers of mouse muscle (Westerblad and Allen, 1991), the rate of loading of fura-2-AM was ~34 μM/h at 22°C, a value somewhat higher than that reported in this article (8 μM/h at 16°C). This discrepancy, however, would probably be reduced substantially if comparable calibration methods had been used to estimate indicator concentrations. The method of Westerblad and Allen, which relies on in vitro fluorescence measurements, likely overestimates intracellular indicator concentration about twofold, since the quantum efficiency of fura-2 is likely to be about twofold larger in the myoplasmic environment than in a simple salt solution (Konishi et al., 1988). In contrast, our absorbance method, which relies on in vitro measurements of extinction coefficients, probably overestimates intracellular indicator concentration by a smaller amount (~25%), since extinction coefficients appear to be less sensitive to alteration by the myoplasmic environment than is quantum efficiency (cf. Konishi et al., 1988). Moreover, the ~25% overestimate inherent in our absorbance calibration is approximately offset by our choice of λ_{ex} with fura-2 (410 nm), since the fura-2 that is in the Ca^{2+}-bound form (~30% in a resting fiber; Lee et al., 1991) is not detected with 410-m excitation.

In their fura-2-AM loading study, Westerblad and Allen (1991) also reported that the peak value of $\Delta F/F$ after AM loading was smaller than that observed after microinjection of fura-2. Their implied f value for fura-2 in mammalian fibers, 0.79, is similar to that which we report for frog fibers, 0.76 (column 9 of Table 2). As noted in Results, our f value for fura-2 is based on average loading times that were rather long (several hours); with shorter loading times, and hence smaller fiber concentrations of indicator, the f value for fura-2 in amphibian fibers may be smaller (cf. Fig. 5). Again, these results suggest caution in the calibration of $[Ca^{2+}]_i$ in AM-loaded cells, especially if cellular concentrations of indicator are substantially smaller than 100 μM.

This work was supported by US National Institutes of Health Grant NS 17620 (to S.M.B.) and grants from the Muscular Dystrophy Association.

REFERENCES

Almers, W., and E. Neher. 1985. The Ca signal from fura-2 loaded mast cells depends strongly on the method of dye-loading. *FEBS Lett.* 192: 13–18.

Baylor, S. M., W. K. Chandler, and M. W. Marshall. 1983. Sarcoplasmic reticulum calcium release in frog skeletal muscle fibres estimated from arsenazo III calcium transients. *J. Physiol.* 344:625–666.

Baylor, S. M., and S. Hollingworth. 1988. Fura-2 calcium transients in frog skeletal muscle fibres. *J. Physiol.* 403:151–192.

Baylor, S. M., and S. Hollingworth. 1990. Absorbance signals from resting frog skeletal muscle fibers injected with the pH indicator dye, phenol red. *J. Gen. Physiol.* 96:449–471.

Baylor, S. M., S. Hollingworth, C. S. Hui, and M. E. Quinta-Ferreira. 1986. Properties of the metallochromic dyes arsenazo III, antipyrylazo III and azo 1 in frog skeletal muscle fibres at rest. *J. Physiol.* 377:89–141.

Baylor, S. M., and H. Oetliker. 1975. Birefringence experiments on isolated skeletal muscle fibres suggest a possible signal from the sarcoplasmic reticulum. *Nature.* 253:97–101.

Cantor, C. R., and P. R. Schimmel. 1980. Biophysical Chemistry. Part II. W. H. Freeman and Co., San Francisco. 439–444.

Caputo, C., K. A. P. Edman, F. Lou, and Y.-B Sun. 1994. Variation in myoplasmic Ca^{2+} concentration during contraction and relaxation studied by the indicator fluo-3 in frog muscle fibres. *J. Physiol.* 478: 137–148.

Claflin, D. R., D. L. Morgan, D. G. Stephenson, and F. J. Julian, 1994. The intracellular Ca^{2+} transient and tension in frog skeletal muscle fibres measured with high temporal resolution. *J. Physiol.* 475:319–325.

Hollingworth, S., and S. M. Baylor. 1990. Changes in phenol red absorbance in response to electrical stimulation of frog skeletal muscle fibers. *J. Gen. Physiol.* 96:473–491.

Hollingworth, S., A. B. Harkins, N. Kurebayashi, M. Konishi, and S. M. Baylor. 1992. Excitation-contraction coupling in intact frog skeletal muscle fibers injected with mmolar concentrations of fura-2. *Biophys. J.* 63:224–234.

Johnson, J. D., and Y. Jiang. 1996. Effect of intracellular calcium (Ca) chelators on Ca transients and relaxation rates in frog skeletal muscle. *Biophys. J.* 70:A248.

Konishi, M., S. Hollingworth, A. B. Harkins, and S. M. Baylor. 1991. Myoplasmic calcium transients in intact frog skeletal muscle fibers monitored with the fluorescent indicator furaptra. *J. Gen. Physiol.* 97: 271–301.

Konishi, M., A. Olson, S. Hollingworth, and S. M. Baylor. 1988. Myoplasmic binding of fura-2 investigated by steady-state fluorescence and absorbance measurements. *Biophys. J.* 54:1089–1104.

Kurebayashi, N., A. B. Harkins, and S. M. Baylor. 1993. Use of fura red as an intracellular calcium indicator in frog skeletal muscle fibers. *Biophys. J.* 64:1934–1960.

Lee, J. A., H. Westerblad, and D. G. Allen. 1991. Changes in tetanic and resting $[Ca^{2+}]_i$ during fatigue and recovery of single muscle fibres from *Xenopus Laevis*. *J. Physiol.* 433:307–326.

Roe, M. W., J. J. Lemasters, and B. Herman. 1990. Assessment of fura-2 for measurements of cytosolic free calcium. *Cell Calcium.* 11:63–73.

Scanlon, M., D. A. Williams, and F. S. Fay. 1987. A Ca^{2+} insensitive form of fura-2 associated with polymorphonuclear leukocytes. Assessment and accurate Ca^{2+} measurement. *J. Biol. Chem.* 262:6308–6312.

Tsien, R. Y. 1981. A non-disruptive technique for loading calcium buffers and indicators into cells. *Nature.* 290:527–528.

Westerblad, H., and D. G. Allen. 1991. Changes of myoplasmic calcium concentrations during fatigue in single mouse muscle fibers. *J. Gen. Physiol.* 8:615–635.

Williams, D. A., and F. S. Fay. 1990. Intracellular calibration of the fluorescent indicator fura-2. *Cell Calcium.* 11:75–83.

Zhao, M., S. Hollingworth, and S. M. Baylor. 1995. AM Loading of calcium indicators into frog skeletal muscle fibers. *Biophys. J.* 68:A418.

Zhao, M., S. Hollingworth, and S. M. Baylor. 1996. Properties of tri- and tetracarboxylate Ca^{2+} indicators in frog skeletal muscle fibers. *Biophys. J.* 70:896–916.